Differential ability of proinflammatory and anti-inflammatory macrophages to perform macropinocytosis

Dar'ya S. Redka[a], Michael Gütschow[b], Sergio Grinstein[a,c,d,*], and Johnathan Canton[a]
[a]Division of Cell Biology, Hospital for Sick Children, Toronto, ON M5G 1X8, Canada; [b]Pharmaceutical Institute, Pharmaceutical Chemistry I, University of Bonn, D-53121 Bonn, Germany; [c]Department of Biochemistry, University of Toronto, ON M5S 1A8, Canada; [d]Keenan Research Centre for Biomedical Science, St. Michael's Hospital, Toronto, ON M5B 1W8, Canada

ABSTRACT **Macropinocytosis mediates the uptake of antigens and of nutrients that dictate the regulation of cell growth by mechanistic target of rapamycin complex 1 (mTORC1). Because these functions differ in proinflammatory and anti-inflammatory macrophages, we compared the macropinocytic ability of two extreme polarization states. We found that anti-inflammatory macrophages perform vigorous macropinocytosis constitutively, while proinflammatory cells are virtually inactive. The total cellular content of Rho-family GTPases was higher in anti-inflammatory cells, but this disparity failed to account for the differential macropinocytic activity. Instead, reduced activity of Rac/RhoG was responsible for the deficient macropinocytosis of proinflammatory macrophages, as suggested by the stimulatory effects of heterologously expressed guanine nucleotide-exchange factors or of constitutively active (but not wild-type) forms of these GTPases. Similarly, differences in the activation state of phosphatidylinositol 3-kinase (PtdIns3K) correlated with the macropinocytic activity of pro- and anti-inflammatory macrophages. Differences in PtdIns3K and Rho-GTPase activity were attributable to the activity of calcium-sensing receptors (CaSRs), which appear to be functional only in anti-inflammatory cells. However, agonists of PtdIns3K, including cytokines, chemokines, and LPS, induced macropinocytosis in proinflammatory cells. Our findings revealed a striking difference in the macropinocytic ability of pro- and anti-inflammatory macrophages that correlates with their antigen-presenting and metabolic activity.**

Monitoring Editor
Jean E. Gruenberg
University of Geneva

Received: Jun 22, 2017
Revised: Oct 16, 2017
Accepted: Oct 27, 2017

INTRODUCTION

Macrophages can exist in a variety of functional states, often distinguished by their proinflammatory or anti-inflammatory properties (Mosser and Edwards, 2008; Mantovani *et al.*, 2013; Patel *et al.*, 2017). This functional versatility is essential for macrophages to fulfill their complex homeostatic, regulatory, and microbicidal roles. Indeed, misregulation of macrophage polarization contributes to infections and autoimmune disorders and to chronic inflammatory diseases such as atherosclerosis, diabetes, and cancer (Jiang *et al.*, 2014; Kaneda *et al.*, 2016; Perl, 2016).

Anti-inflammatory macrophages, often referred to as alternatively activated or M2-like, scan for danger signals and maintain tissue homeostasis. Proinflammatory macrophages, generally referred to as classically activated or M1-like, are responsible for killing pathogens and presenting their antigens to the adaptive immune system. Subsequently, the anti-inflammatory cells clear the inflammation and repair damaged tissues (Das *et al.*, 2015). Recognition of danger signals and tuning of the macrophage response involves pattern-recognition receptors (PRRs), which are located in various cellular compartments. Some, like Toll-like receptors (TLRs) 2 or 4 are present at the plasma membrane, while TLR3, 7, 8, and 9 are

This article was published online ahead of print in MBoC in Press (http://www.molbiolcell.org/cgi/doi/10.1091/mbc.E17-06-0419) on November 1, 2017.

*Address correspondence to: Sergio Grinstein (sergio.grinstein@sickkids.ca).

Abbreviations used: CA, constitutively active; CaSR, calcium-sensing receptor; GEF, guanine nucleotide exchange factor; GM-CSF, granulocyte macrophage colony-stimulating factor; GM/IFN-γ/LPS-cultured, cultured in GM-CSF, interferon-γ, and lipopolysaccharide; hMDM, human monocyte-derived macrophages; IFN-γ, interferon-γ; IL-4, interleukin-4; LPS, lipopolysaccharide; M-CSF, macrophage colony-stimulating factor; M/IL4-cultured, cultured in M-CSF and IL-4; mTOR, mechanistic target of rapamycin; PRR, pattern-recognition receptors; PtdIns3K, phosphatidylinositol 3-kinase; RT-PCR, reverse transcription-PCR; sGEF, SH3-containing GEF; Tiam1, T-cell lymphoma invasion and metastasis-inducing protein 1; TLR, Toll-like receptor; TMR, tetramethylrhodamine.

localized primarily in endolysosomal compartments (Barton and Kagan, 2009; De Nardo, 2015). Macrophages can internalize pathogens, thereby delivering ligands to PRRs in intracellular compartments of PRRs, via two pathways: phagocytosis, which mediates the uptake of particulate targets, and macropinocytosis, a distinct process that enables the internalization of soluble signals. By trapping soluble PRR ligands released by pathogens, macropinocytosis enables early signaling by macrophages distant from the sites of infection.

Macropinocytosis, the uptake of extracellular fluid into large (>250 nm) vacuoles called macropinosomes, is an actin- and phosphatidylinositol 3-kinase (PtdIns3K)–dependent process (Swanson, 2008; Kerr and Teasdale, 2009). In certain cells types, macropinocytosis can be triggered by growth signals or chemokines for nutrient uptake during development and cancer (Bloomfield and Kay, 2016), recycling of adhesion receptors during cell migration (Gu *et al.*, 2011), or for membrane retrieval during neuronal growth (Holt *et al.*, 2003). Such macropinocytosis will be referred to hereafter as the induced type. In dendritic cells and macrophages, however, where macropinocytosis is thought to play a role in PRR ligand uptake and antigen presentation (Swanson, 2008; Lim and Gleeson, 2011), macropinocytosis occurs continuously in the ostensible absence of stimulation by growth factors or chemokines. In nonpolarized human monocyte-derived macrophages (hMDMs), this type of "constitutive" macropinocytosis was shown to be mediated by calcium-sensing receptors (CaSRs; Canton *et al.*, 2016).

Considering the different functional roles of proinflammatory and anti-inflammatory macrophages, we wondered whether macropinocytosis operates similarly in differentially polarized macrophages. To this end, we compared the constitutive macropinocytic activity of hMDMs polarized toward the proinflammatory (M1-like) phenotype using granulocyte macrophage colony-stimulating factor (GM-CSF) followed by interferon-γ (IFN-γ) and lipopolysaccharide (LPS), with that of anti-inflammatory (M2-like) cells generated using macrophage colony-stimulating factor (M-CSF) followed by interleukin-4 (IL-4). We also assessed whether macropinocytosis could be induced acutely in these cells by the addition of cytokines, chemokines, or LPS. Our analysis revealed striking differences in the macropinocytic activity of both polarization states, prompting us to investigate the molecular basis of this contrasting behavior.

RESULTS

Analysis of constitutive macropinocytosis in polarized macrophages

Dendritic cells and macrophages are known to carry out macropinocytosis constitutively, i.e., in the absence of ostensible stimulation (Sallusto *et al.*, 1995; Lim and Gleeson, 2011; Canton *et al.*, 2016). The effect of polarization on macropinocytic activity, however, has not been established. To this end, proinflammatory macrophages were generated by exposing human blood monocytes to GM-CSF for 5 d, followed by treatment with IFN-γ and LPS for an additional 2 d. These cells are referred to hereafter as GM/IFN-γ/LPS–cultured. Anti-inflammatory macrophages were induced by exposing monocytes to M-CSF, followed by IL-4 and are referred to as M/IL4-cultured cells. The occurrence of polarization was validated assessing the expression of two canonical proinflammatory cell-surface markers, CD40 and CD80, and two anti-inflammatory markers, CD163 and CD200R (Jaguin *et al.*, 2013; Vogel *et al.*, 2014) by flow cytometry. On day 7, GM/IFN-γ/LPS–cultured cells had high levels of CD40 and CD80, whereas expression of these markers was low in M/IL4-cultured cells (Figure 1, Supplemental Figure S1, and Supplemental Table S1). Conversely, the anti-inflammatory markers CD163 and CD200R were

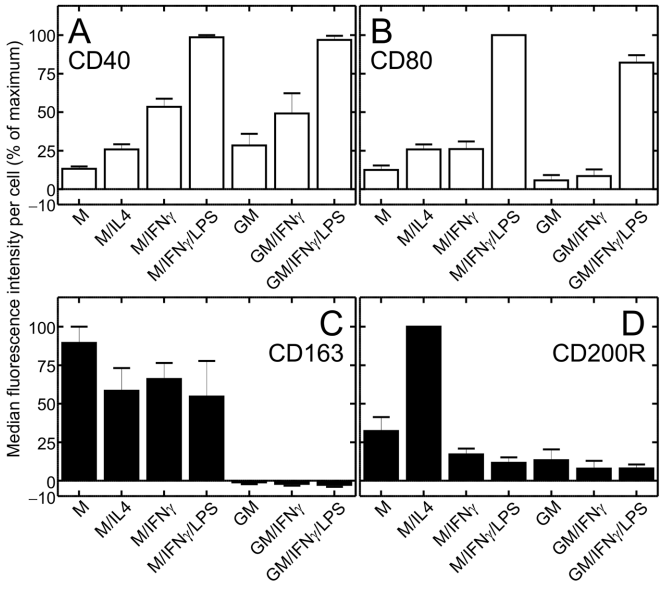

FIGURE 1: Cell-surface expression of pro- and anti-inflammatory markers in macrophages cultured under various conditions. Human blood monocytes were cultured for 5 d as described in *Materials and Methods* in either M-CSF (columns 1–4) or GM-CSF (columns 5–7), followed by 2 more days in either M-CSF (M) or GM-CSF (GM) alone, or in the additional presence of either IL-4 (M/IL4), IFN-γ (M/IFN-γ and GM/IFN-γ), or a combination of IFN-γ and LPS (M/IFN-γ/LPS and GM/IFN-γ/LPS). Cells were then lifted and labeled with either FITC-conjugated anti-human CD40 (a proinflammatory marker; A), APC-conjugated anti-human CD80 (a proinflammatory marker; B), Alexa-647-conjugated anti-human CD163 (an anti-inflammatory marker; C), or PE-conjugated anti-human CD200R antibody (an anti-inflammatory marker; D). Cell-surface labeling was determined by flow cytometry. Similarly labeled isotype-matched (κ) controls were used to subtract nonspecific labeling (shown in Supplemental Figure S1). Data are means (± SEM) of median fluorescence intensity per cell, minus the signal from the corresponding isotype control, normalized to the highest median fluorescence intensity per experiment, from 15,400 to 19,700 cells in three independent experiments of each type, with blood from three donors. Representative fluorescence intensity histograms are shown in Supplemental Figure S1. Probabilities of statistical significance for comparisons between all pairs of data sets are presented as a matrix in Supplemental Table S1.

clearly expressed in M/IL4-cultured cells yet were barely detectable in GM/IFN-γ/LPS–cultured cells. Measuring CD1a expression, we had confirmed previously that these protocols yield preparations devoid of dendritic cells (Canton *et al.*, 2014).

The pro- and anti-inflammatory cells generated as above differed also in their appearance. In accordance with earlier findings (McWhorter *et al.*, 2013), the GM/IFN-γ/LPS–cultured cells displayed a round and flattened ("fried-egg") morphology, while M/IL4-cultured cells were elongated (Figure 2A).

To examine the ability of GM/IFN-γ/LPS– and M/IL4-cultured macrophages to perform macropinocytosis constitutively, we measured the uptake of tetramethylrhodamine (TMR)-labeled 70 kDa dextran in otherwise unstimulated cells. As shown in Figure 2B, M/IL4-cultured macrophages took up large amounts of the 70 kDa dextran, generating on average 46 macropinosomes (defined as vacuolar structures of diameter ≥0.8 μm) per cell in 15 min. In sharp contrast, macropinosomes were rarely found in the GM/IFN-γ/LPS–cultured macrophages; after a comparable incubation less than one macropinosome per cell was observed (Figure 2, B and C).

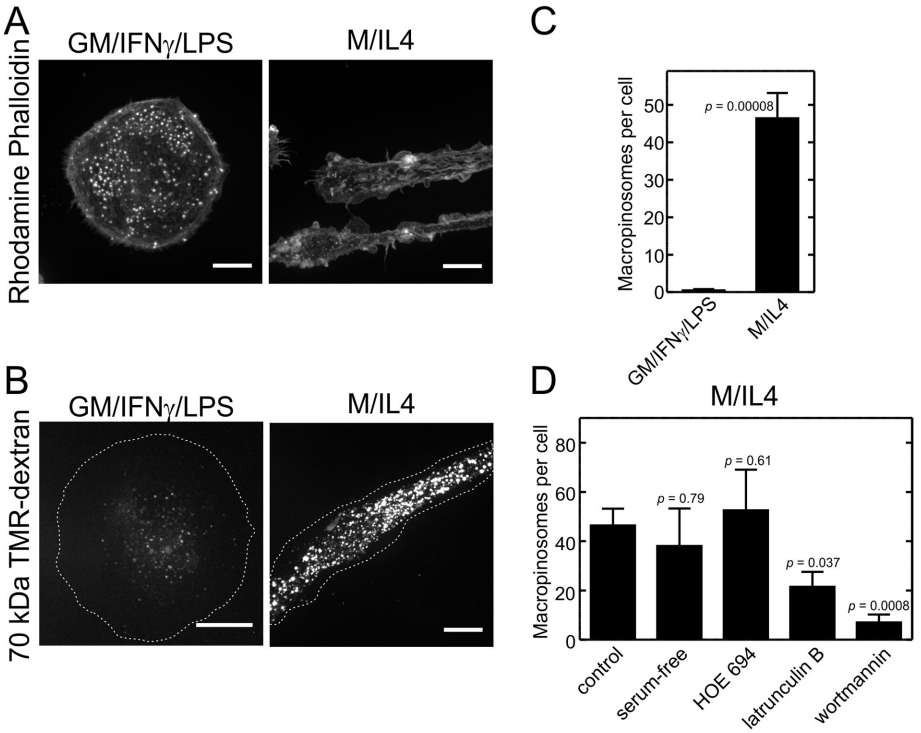

FIGURE 2: Differential macropinocytic activity and actin structure of GM/IFN-γ/LPS– vs. M/IL4-cultured macrophages. (A) GM/IFN-γ/LPS– (left) and M/IL4-cultured (right) macrophages were fixed, permeabilized, and labeled with fluorescent phalloidin. (B) GM/IFN-γ/LPS– (left) and M/IL4-cultured (right) macrophages were incubated with fluorescently labeled 70 kDa dextran (TMR-dextran, 125 μg/ml) for 15 min at 37°C in calcium-containing medium. Cells were then washed, fixed, and imaged immediately by spinning disk confocal microscopy. (C) The number of macropinosomes (i.e., TMR-positive vacuoles) per cell was counted from 2D projections of 3D stacks using ImageJ software, applying a lower particle area threshold of 0.5 μm^2. (D) M/IL4-cultured macrophages were pretreated with HOE 694 (10 μM, 30 min), latrunculin B (2 μM, 30 min), or wortmannin (100 nM, 15 min) and then incubated with fluorescently labeled 70 kDa dextran (TMR-dextran, 125 μg/ml) for 15 min at 37°C in calcium-containing medium with the respective drugs present. In the case of latrunculin B and wortmannin, the pretreatment medium was serum-free, and a serum-free medium with no treatment was used as a control for those experiments (column 2). Cells were then washed, fixed, and imaged immediately by spinning disk confocal microscopy. The number of macropinosomes (i.e., TMR-positive vacuoles) per cell then was determined as described for C. Typical images (A, B) and quantifications (C, D; means ± SEM) are representative of 30–60 cells from three to six experiments of each type using blood from at least two different donors. Scale bars, 15 μm.

It was shown previously that 70 kDa dextran is internalized almost exclusively via macropinosomes, as it is excluded by smaller-sized endocytic pathways such as clathrin-coated vesicles or caveolae (Li *et al.*, 2015). This was confirmed to be the case also for nonpolarized human hMDMs, where uptake of the large dextran was virtually eliminated by latrunculin—the prototypical inhibitor of macropinocytosis—under conditions where the uptake of transferrin (a marker of clathrin-mediated uptake) was unaffected (Canton *et al.*, 2016). To ensure that the probe used was entering the cells through fluid-phase, as opposed to adsorptive uptake, M/IL4-cultured cells were incubated with the labeled dextran for 15 min at 4°C, followed by its removal from the medium and incubation for an additional 15 min at 37°C. Under these conditions, uptake of dextran was negligible (Supplemental Figure S2, A and B). In addition, after coincubation at 37°C for 15 min, the small fluorescent molecule Lucifer Yellow, which is structurally different from dextran and hence unlikely to adsorb onto the same sites, filled the same large vacuoles as the 70 kDa dextran (Supplemental Figure S2, C and D). Together, these observations confirm that 70 kDa TMR-dextran is internalized via fluid-phase uptake, rather than via an adsorptive mechanism.

Both induced and constitutive forms of macropinocytosis are known to be PtdIns3K- and actin-dependent (Araki *et al.*, 1996; Zhou *et al.*, 1998; Amyere *et al.*, 2000; Hoeller *et al.*, 2013). To confirm that the vacuoles formed constitutively by the M/IL4-cultured cells were bona fide macropinosomes, we tested the effects of wortmannin (a PtdIns3K inhibitor) and latrunculin B. Both of these agents markedly reduced the number of macropinosomes in M/IL4-cultured macrophages (Figure 2D). Interestingly, while amiloride and its analogues are potent inhibitors of macropinocytosis in several systems (West, 1989; Dowrick *et al.*, 1993; Canton *et al.*, 2016), HOE-694 was without effect on M/IL4-cultured cells (Figure 2C), replicating the results obtained in other myeloid cells (Norbury *et al.*, 1997; Canton *et al.*, 2016).

Macropinocytic activity of macrophages with intermediate phenotypes

Differentiation of macrophages with GM/IFN-γ/LPS or M/IL4 gives rise to two extreme phenotypes: fully pro- and anti-inflammatory, respectively. Others have used less extreme culture conditions to polarize macrophages, some of which yield intermediate phenotypes. We therefore assessed the macropinocytic ability of cells subjected to a range of differentiation protocols (detailed in *Materials and Methods*), namely, 1) M-CSF alone (M); 2) M-CSF followed by IFN-γ (M/IFN-γ); 3) M-CSF followed by IFN-γ and LPS (M/IFN-γ/LPS); 4) GM-CSF only (GM); and 5) GM-CSF followed by IFN-γ (GM/IFN-γ). To verify the effects of these individual protocols on polarization we measured the expression of proinflammatory markers (CD40 and CD80; Figure 1, A and B) and anti-inflammatory markers (CD80 and CD200R; Figure 1, C and D; Jaguin *et al.*, 2013; Vogel *et al.*, 2014) on day 7 of differentiation. The expression of CD40 was comparatively low with M-CSF alone, but increased 4.0-fold and 7.4-fold if IFN-γ or a mixture of IFN-γ and LPS, respectively, were also present (Figure 1A; see Supplemental Table S1 for probabilities of statistical significance for pairwise comparisons). A similar pattern was observed with GM-CSF–cultured cells (Figure 1A). The expression of CD80 was elevated primarily in response to LPS (3.8-fold relative to M/IFN-γ; 9.6-fold relative to GM/IFN-γ), regardless of the growth factor added (Figure 1B and Supplemental Table S1). Expression of the anti-inflammatory marker CD163 was apparent in all protocols that contained M-CSF, whereas it was fully suppressed in all preparations that contained GM-CSF (Figure 1C). Lastly, expression of CD200R was significantly elevated only in response to IL-4 (Figure 1D). Together, these results confirm that preparations cultured with IFN-γ and/or LPS developed

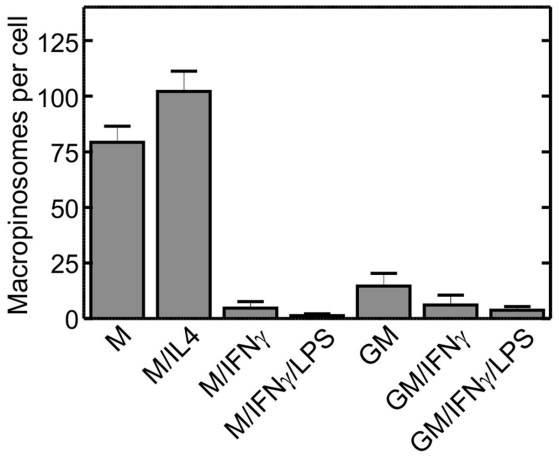

FIGURE 3: Macropinocytic activity of macrophages cultured under various conditions. Human blood monocytes were cultured for 5 d in either M-CSF (columns 1–4) or GM-CSF (columns 5–7), followed for 2 more days in either M-CSF (M) or GM-CSF (GM) alone, or in the additional presence of either IL-4 (M/IL4), IFN-γ (M/IFN-γ and GM/IFN-γ), or a combination of IFN-γ and LPS (M/IFN-γ/LPS and GM/IFN-γ/LPS), as described in *Materials and Methods*. On day 7 cells were incubated with fluorescently labeled 70 kDa dextran (TMR-dextran, 125 μg/ml) for 15 min at 37°C in calcium-containing medium. Cells were then washed, fixed, and imaged immediately by spinning disk confocal microscopy. The number of macropinosomes (i.e., TMR-positive vacuoles) per cell then was determined as described for Figure 2C. Data are means ± SEM of 30–75 cells from three to seven experiments of each type using blood from at least three different donors. Probabilities of statistical significance for comparisons between all pairs of data sets are presented as a matrix in Supplemental Table S2.

proinflammatory properties, while those cultured in M-CSF with or without IL-4 acquired (at least some) anti-inflammatory properties, which were in turn suppressed by GM-CSF. As anticipated, the combination of GM/IFN-γ/LPS yielded the most pronounced proinflammatory, whereas M/IL4-cultured macrophages displayed the most consistent anti-inflammatory phenotype.

Next, we examined the macropinocytic activity of these differently polarized macrophages. As illustrated in Figure 3, both M- and M/IL4-cultured macrophages exhibited a considerably higher macropinocytic activity than the other preparations (e.g., 15- and 7-fold higher, respectively, than GM-cultured cells; see Table S2 for probabilities of statistical significance for pairwise comparisons). GM-CSF was insufficient to elicit macropinocytosis, while IFN-γ and/or LPS suppressed the stimulatory effect of M-CSF. It appears, therefore, that the macropinocytic phenotype is associated with an anti-inflammatory phenotype. To further analyze the mechanism underlying the differential macropinocytic activity, we therefore proceeded to use the two most contrasting phenotypes: GM/IFN-γ/LPS– versus M/IL4-cultured cells.

Rho GTPases are more abundant and more active in M/IL4- than in GM/IFN-γ/LPS–cultured macrophages

Morphological differences between the GM/IFN-γ/LPS– and M/IL4-cultured macrophages pointed to a distinct cytoskeletal arrangement, which was validated by staining F-actin with phalloidin (Figure 2A). Whereas GM/IFN-γ/LPS–cultured cells displayed a continuous band of cortical actin on their dorsal membrane and multiple ventral podosomes, M/IL4-cultured cells had florid dorsal ruffles and few podosomes. We reasoned that these profound differences may be attributable to differential content and/or activity of Rho-family GTPases, which dictate the assembly of F-actin. The abundance of Rac1, RhoA, RhoG, and Cdc42 was compared in the two polarization states by immunoblotting, normalizing the data to the actin content. Remarkably, M/IL4-cultured macrophages expressed higher levels of the four tested Rho GTPases, the difference being greatest for Rac1 (Figure 4A; see Supplemental Figure S3A for representative blots).

To determine whether the differential expression of the Rho GTPases resulted in their differential activity, the GTP-bound (i.e., active) form of each of the G proteins was measured using either a G-LISA (for Rac1, RhoA, and Cdc42) or a pull-down assay (for RhoG; Figure 4B and Supplemental Figure S3B). Rac1 and RhoG were significantly more active in M/IL4- than in GM/IFN-γ/LPS–cultured cells, while the differences detected in the case of RhoA and Cdc42 were not statistically significant (Figure 4B).

Activation—but not overexpression—of Rac1 or RhoG confer constitutive macropinocytic activity to GM/IFN-γ/LPS–cultured macrophages

Considering that M/IL4-cultured macrophages express substantially greater levels of Rac1 and to a lesser extent RhoA, RhoG, and Cdc42 (Figure 4A), we tested whether ectopic overexpression of any of the GTPases would confer the constitutive macropinocytic ability to GM/IFN-γ/LPS–cultured cells. Fluorescently tagged versions of the wild-type form of the GTPases were used to verify their expression following transient transfection of GM/IFN-γ/LPS–cultured macrophages. As shown in Figure 4C, none of the GTPases increased macropinocytosis significantly in the GM/IFN-γ/LPS–cultured cells. The lower abundance of Rho GTPases in the GM/IFN-γ/LPS–cultured cells is therefore unlikely to account for their reduced macropinocytic effectiveness.

We next considered whether insufficient activation rather than differential expression of the GTPases was responsible for the reduced macropinocytosis of GM/IFN-γ/LPS–cultured cells. This possibility was assessed expressing constitutively active (CA) forms of the GTPases; as before, fluorescently tagged constructs were used to identify transfectants. Transfection of GM/IFN-γ/LPS–cultured macrophages with either CA-Rac1 (Rac1-Q61L-GFP [green fluorescent protein]) or CA-RhoG (RhoG-G12V-CFP) resulted in a striking increase in macropinocytosis, exceeding the constitutive levels observed in the M/IL4-cultured macrophages (Figure 4, D and E). CA-Cdc42 (Cdc42-G12V-YFP) effected a much smaller, yet significant, increase, whereas CA-RhoA (RhoA-Q63L-GFP) was without effect (Figure 4E).

Together, these results indicate that availability of active Rac1 and/or RhoG, as opposed to the total level of expression of the GTPases, limit the ability of GM/IFN-γ/LPS–cultured cells to perform constitutive macropinocytosis. This notion was validated by heterologous overexpression of guanine nucleotide exchange factors (GEFs) that can activate the endogenous GTPases. To activate Rac1 we used T-cell lymphoma invasion and metastasis-inducing protein 1 (Tiam1), which has been shown to localize to the membrane in macrophages (Bohdanowicz *et al.*, 2013). SH3-containing GEF (sGEF) was used to stimulate RhoG; of note, sGEF was shown to be involved in macropinocytosis in epithelial cells (Ellerbroek *et al.*, 2004). As illustrated in Figure 4, D and E, both GEFs caused a remarkable increase in the number of macropinosomes, reminiscent of the effects of the CA mutants of Rac1 and RhoG. These results suggest that, regardless of the lower expression levels detected in GM/IFN-γ/LPS–cultured cells, the amount of Rac1 and RhoG expressed by GM/IFN-γ/LPS–cultured macrophages suffices to support active macropinocytosis.

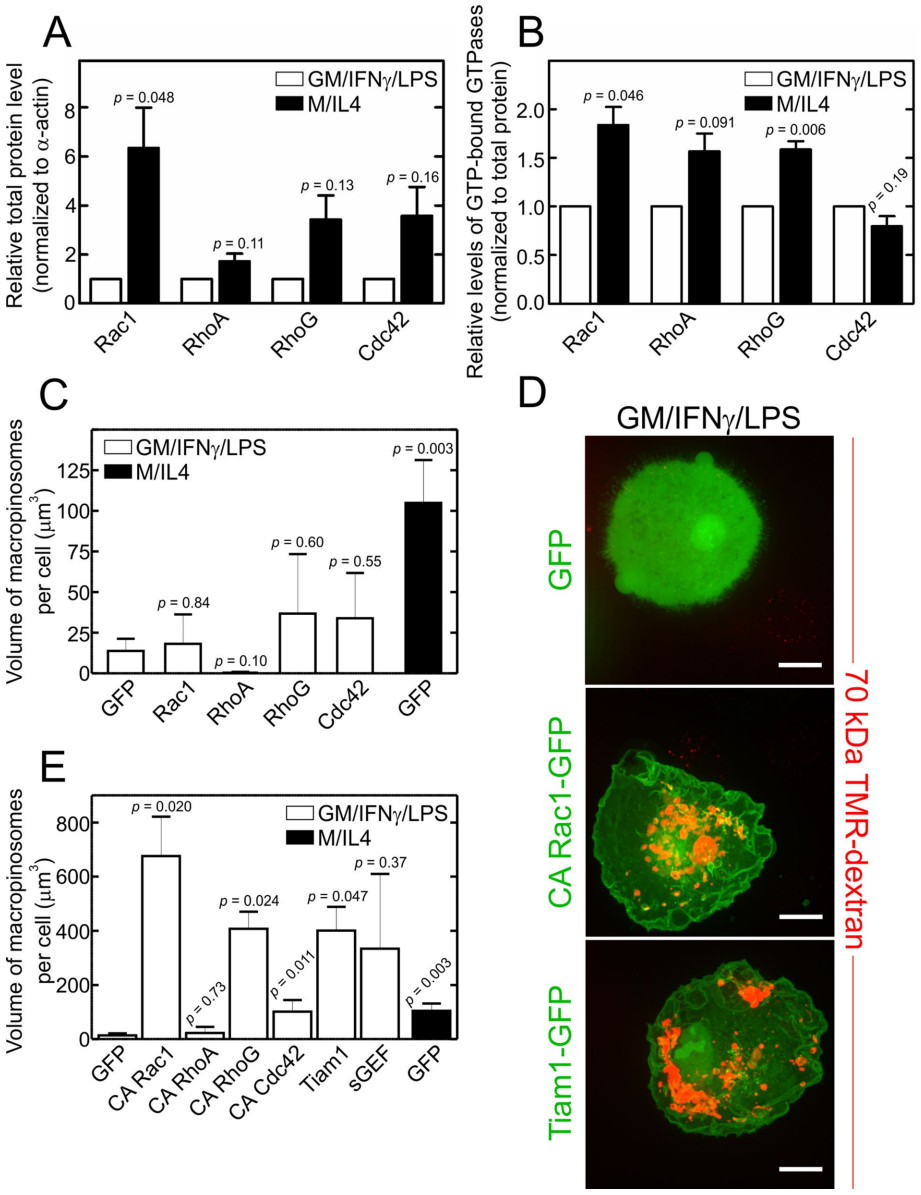

FIGURE 4: Abundance, overexpression, and activation of Rho GTPases in GM/IFN-γ/LPS– and M/IL4-cultured macrophages. (A) GM/IFN-γ/LPS– and M/IL4-cultured macrophages were lysed, separated by 10% SDS–PAGE, and subjected to immunoblotting with anti-Rac1, anti-RhoA, anti-RhoG, or anti-Cdc42 antibodies. Intensities of the bands were normalized to β-actin, and then plotted as a ratio relative to GM/IFN-γ/LPS–cultured macrophages in each experiment for each GTPase. Data are means ± SEM of three to four independent experiments. Typical immunoblots are shown in Supplemental Figure S3A. (B) GM/IFN-γ/LPS– and M/IL4-cultured macrophages were lysed, followed immediately by measurement of the GTP-bound form of Rac1, RhoA, and Cdc42 using the respective colorimetric G-LISA kit. The measured absorbance at 490 nm was normalized to total protein levels and plotted as a ratio relative to GM/IFN-γ/LPS–cultured macrophages in each experiment for each GTPase. Data are means ± SEM of three to four independent experiments. Levels of GTP-bound RhoG in lysed GM/IFN-γ/LPS– and M/IL4-cultured macrophages were measured using a pull-down assay with a recombinant ELMO-GST loaded onto glutathione-sepharose beads, followed by 10% SDS–PAGE and immunoblotting with an anti-RhoG antibody. Levels of RhoG.GTP were normalized relative to the level in GM/IFN-γ/LPS–cultured macrophages in each experiment. A typical immunoblot for the RhoG.GTP pull-down assay is shown in Supplemental Figure S3B. Data are means ± SEM from four independent experiments. *C. difficile* toxin B treatment (3 h in serum-free medium) was used to inhibit all four GTPases, i.e., as a negative control, in all G-LISA and RhoG.GTP pull-down assays. (C–E) GM/IFN-γ/LPS–cultured macrophages were transfected with fluorescently tagged constructs of either wild-type (C) or constitutively active Rac1, RhoA, RhoG, or Cdc42 (D, E), or of the Rac1 and RhoG GEFs Tiam1 and sGEF, as indicated (D, E). The specific constructs used were Rac1-GFP, RhoA-GFP, RhoG-CFP, Cdc42-GFP, Rac1-Q61L-GFP, RhoA-Q63L-GFP, RhoG-G12V-CFP, Cdc42-G12V-YFP, Tiam1-GFP, and sGEF-GFP. GM/IFN-γ/LPS–cultured macrophages transfected with GFP alone were used as a negative control, while M/IL4-cultured macrophages transfected with GFP alone were used as a positive control. After 24-h transfection, the cells were incubated with fluorescently labeled 70 kDa dextran (TMR-dextran, 125 μg/ml) for 15 min at 37°C, and washed, fixed, and imaged immediately (D); only transfected cells were selected for measurements of macropinocytosis, which was quantified (C, E) as the total volume of TMR-positive vacuoles per cell from 3D stacks using 3D particle analysis in ImageJ software, applying a lower particle volume threshold of 0.26 μm^3. Typical images (D) and quantifications (C, E; means ± SEM) are representative of 20–50 cells from three to five independent experiments using blood from at least two separate donors. Scale bars, 15 μm.

PtdIns3K is less active in the GM/IFN-γ/LPS–cultured macrophages

The preceding data indicate that the ineffective activation of Rac1 and RhoG curtails the ability of GM/IFN-γ/LPS–cultured cells to form macropinosomes, suggesting insufficient GEF activity. Several Rho-family GEFs are recruited and/or activated by PtdIns(3,4,5)P_3, and this phosphoinositide is essential for macropinocytosis. We therefore considered the possibility that reduced PtdIns(3,4,5)P_3 generation may be responsible for the poor ability of GM/IFN-γ/LPS–cultured cells to perform constitutive macropinocytosis. To that end, we used a fluorescently labeled PH domain of Akt [PH(Akt)-GFP] to compare the abundance and distribution of PtdIns(3,4,5)P_3 in GM/IFN-γ/LPS– and M/IL4-cultured cells. In M/IL4-cultured macrophages, the biosensor associated with the inner leaflet of the plasma membrane, making its fluorescence intensity significantly greater than that of the cytosol (Figure 5, A and B). That this reflected the constitutive presence of PtdIns(3,4,5)P_3 was indicated by the effect of wortmannin, which caused the release of the membrane-associated PH(Akt)-GFP, increasing the cytosolic fluorescence intensity. In contrast, no preferential association of the probe with the membrane was discernible in most GM/IFN-γ/LPS–cultured cells.

The activity of PtdIns3K was also compared in the two types of macrophages by quantifying the phosphorylation of Akt, which is known to vary in proportion to the PtdIns(3,4,5)P_3 content. Immunoblotting revealed that Akt is phosphorylated to a greater extent in M/IL4- than in

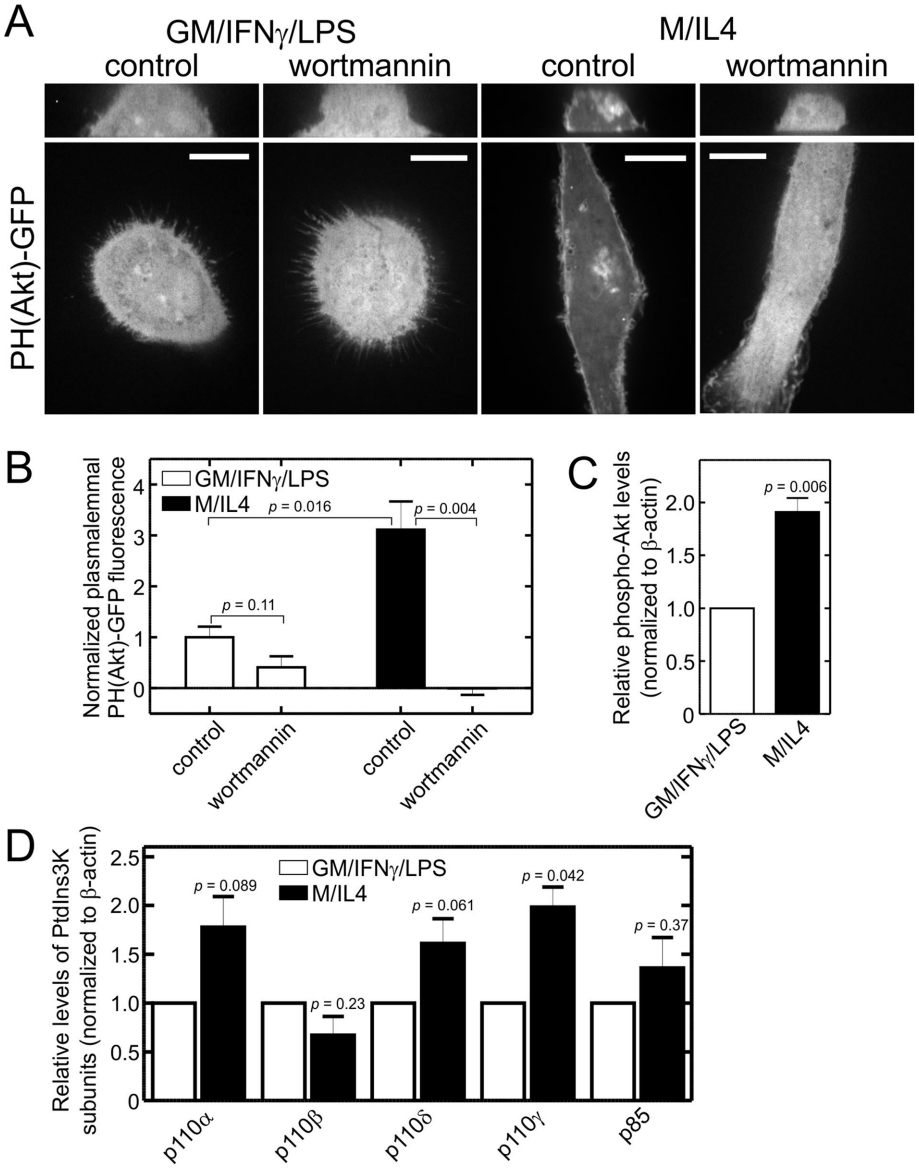

FIGURE 5: PtdIns3K is less active and less abundant in GM/IFN-γ/LPS–cultured macrophages. (A) GM/IFN-γ/LPS– and M/IL4-cultured macrophages were transfected with PH(Akt)-GFP, a biosensor of PtdIns(3,4,5)P_3, and imaged live 24 h later, before and after treatment with wortmannin (100 nM, 15 min). Scale bars, 15 μm. (B) Localization of PH(Akt)-GFP to the plasma membrane was quantified as a fractional difference in the mean gray intensity value per pixel of an area selected around the edge of the cell in the middle section of a 3D stack ($Mean_{PM}$) and the mean gray intensity value per pixel of an area in cytoplasm ($Mean_{cytoplasm}$), i.e., ($Mean_{PM}$–-$Mean_{cytoplasm}$)/$Mean_{cytoplasm}$, and normalized to the average value for GM/IFN-γ/LPS–cultured control taken as 1. Data are means ± SEM of 20–40 cells from three to four independent experiments. (C) GM/IFN-γ/LPS– and M/IL4-cultured macrophages were lysed, separated by 10% SDS–PAGE and subjected to immunoblotting with an anti-phospho-Akt antibody. Intensities of the bands were normalized to β-actin, and then plotted as a ratio relative to GM/IFN-γ/LPS–cultured macrophages in each experiment; means ± SEM of four independent experiments are plotted. A representative immunoblot is shown in Supplemental Figure S4A. (D) GM/IFN-γ/LPS– and M/IL4-cultured macrophages were lysed, separated by 10% SDS–PAGE and subjected to immunoblotting with anti-p110α, anti-p110β, anti-p110δ, anti-p110γ, or anti-p85 antibody. Intensities of the bands were normalized to β-actin, and then plotted relative to GM/IFN-γ/LPS–cultured macrophages in each experiment. Data are means ± SEM of three to six independent experiments. Typical immunoblots are shown in Supplemental Figure S4B.

GM/IFN-γ/LPS–cultured macrophages (Figure 5C and Supplemental Figure S4A), in good accordance with the results obtained with the PtdIns(3,4,5)P_3 biosensor.

We next measured the relative abundance of isoforms of the class I PtdIns3K to establish whether the increased activity of M/IL4- compared with GM/IFN-γ/LPS–cultured cells is attributable to differential expression of the enzyme. We quantified the amount of catalytic (p110α, p110β, p110δ, and p110γ) and regulatory (p85) subunits of the kinase in GM/IFN-γ/LPS– and M/IL4-cultured macrophages by immunoblotting (Figure 5D and Supplemental Figure S4B). Expression of p110γ subunit was significantly (≈2.0-fold) higher in the M/IL4-cultured cells, while only smaller, statistically insignificant differences were noted for the p110α, p110β, p110δ, and p85 subunits (Figure 5D).

Recruitment of the p85 regulatory subunit of PtdIns3K to the plasma membrane induces macropinocytosis in GM/IFN-γ/LPS–cultured macrophages

The preceding results suggest that the reduced activity of PtdIns3K in GM/IFN-γ/LPS–cultured cells and their failure to perform constitutive macropinocytosis may result from the lower expression of the p110γ catalytic subunit of PtdIns3K. However, insufficient activation of its regulatory subunit could equally explain the observations. To distinguish between these alternatives, we used a rapamycin-inducible heterodimerization system to steer the p85 subunit of PtdIns3K to the plasma membrane (Figure 6A). GM/IFN-γ/LPS– and M/IL4-cultured macrophages were cotransfected with two constructs: 1) a domain of FK506-binding protein (FKBP) fused to the p85 subunit and a cyan florescent protein (CFP), and 2) the FKBP-rapamycin binding (FRB) domain of mechanistic target of rapamycin (mTOR) fused to the N-terminal 11 amino acids of Lyn kinase, which target the fusion protein to the plasma membrane. Before the addition of rapamycin, FKBP-p85-CFP was mostly cytosolic, but was translocated to the plasma membrane within minutes of the addition of rapamycin (Figure 6B for GM/IFN-γ/LPS–cultured cells; M/IL4-cultured cells not shown). The effect of translocation of p85 to the plasma membrane on the activity of PtdIns3K was verified using the biosensor of PtdIns(3,4,5)P_3, [PH(Akt)-RFP]. In the GM/IFN-γ/LPS–cultured macrophages translocation of p85 to the plasma membrane resulted in a 2.5-fold increase in the plasmalemmal PH(Akt)-RFP, whereas only a smaller, insignificant increase was observed in the M/IL4-cultured cells (Figure 6C).

The increase in PtdIns(3,4,5)P_3 induced by recruitment of p85 to the membrane afforded us the opportunity to assess whether scarcity of the phosphoinositide was the explanation for the inability of

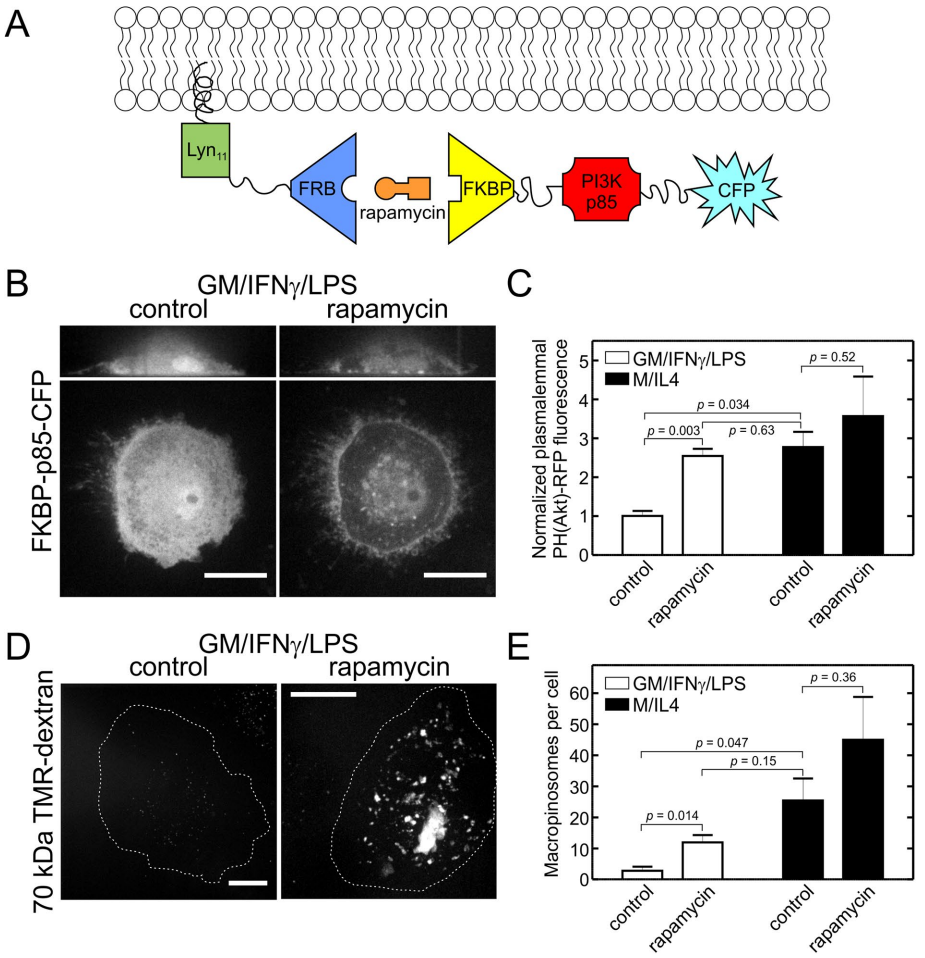

FIGURE 6: Recruitment of the p85 domain of PtdIns3K to the plasma membrane increases macropinocytic activity of GM/IFN-γ/LPS–cultured macrophages. (A) Schematic showing the recruitment of p85-CFP to the plasma membrane via the rapamycin-inducible heterodimerization system. (B, C) GM/IFN-γ/LPS– and M/IL4-cultured macrophages were cotransfected with FKBP-p85-CFP, Lyn_{11}-FRB, and PH(Akt)-RFP. Transfected cells were imaged (B) 24 h posttransfection either before (left) and after (right) addition of rapamycin (1 μM, 15 min; the same cell is shown on the left and right), and the activation PtdIns3K was quantified as redistribution of PH(Akt)-RFP, a biosensor of PtdIns(3,4,5)P_3, to the plasma membrane (C), quantified as described for PH(Akt)-GFP in Figure 5B. Typical images (B) and quantifications (C; means ± SEM) are representative of 20–30 cells from three to four independent experiments. (D, E) GM/IFN-γ/LPS– and M/IL4-cultured macrophages were cotransfected with FKBP-p85-CFP and Lyn_{11}-FRB. After a 24-h transfection, the cells were incubated with fluorescently labeled 70 kDa dextran (TMR-dextran, 125 μg/ml) for 15 min at 37°C, with or without concurrent treatment with rapamycin (1 μM). Cells were then washed, fixed, and imaged immediately (D). Cells positive for CFP were selected for measurements of macropinocytosis, which was quantified as described for Figure 2C (E). Representative images (D) and quantification (means ± SEM; E) of 30–50 cells from three to five independent experiments. Scale bars, 15 μm.

GM/IFN-γ/LPS–cultured cells to perform macropinocytosis. As illustrated in Figure 6, D and E, stimulation of PtdIns(3,4,5)P_3 synthesis by rapamycin-mediated recruitment of p85 markedly activated the macropinocytic activity of GM/IFN-γ/LPS–cultured cells. Stimulation was also observed in M/IL4-cultured cells, although the net effect was not statistically significant due to the varying magnitude of the response. Rapamycin has been reported to depress macropinocytosis (Sallusto *et al.*, 1995; Hackstein *et al.*, 2002), ostensibly by inhibiting mTOR. However, at the concentrations and times used in our experiments, rapamycin did not alter the macropinocytic activity of the nontransfected M/IL4-cultured macrophages in the experiments presented in Figure 6E (unpublished data). Therefore, the observed changes in macropinocytosis resulted from the induction of heterodimerization of the two constructs, and were not caused by rapamycin itself.

Together, the preceding results indicate that, despite their lower expression, sufficient amounts of the catalytic subunits of PtdIns3K are present in GM/IFN-γ/LPS–cultured cells to support macropinocytosis, and that inadequate activation underlies their inability to form macropinosomes.

The constitutive activity of PtdIns3K in M/IL4-cultured macrophages is attributable to CaSR

We recently showed that constitutive macropinocytosis in nonpolarized hMDMs is stimulated by the calcium-sensing receptor, CaSR (Canton *et al.*, 2016). This serpentine receptor is potentially capable of activating the p110β and p110γ subunits of PtdIns3K via a heterotrimeric G protein, likely G_i. It was therefore conceivable that the constitutive macropinocytosis observed in macrophages polarized toward the anti-inflammatory phenotype was similarly mediated by CaSR. This possibility was tested by a) removing extracellular calcium (the ligand responsible for activation of CaSR); b) addition of NPS 2143, a specific CaSR antagonist; c) pretreatment of the cells with pertussis toxin, an inhibitor of $G\alpha_i$; and d) addition of BIM 46187, a pan-G protein inhibitor. As reported in Figure 7A, every one of these treatments markedly inhibited the constitutive macropinocytic activity of M/IL4-cultured macrophages, consistent with the involvement of CaSR and the $G\alpha_i$ protein in the process.

Because macropinocytic activity in polarized macrophages was proportional to the level of PtdIns(3,4,5)P_3, we examined whether the constitutive PtdIns3K activity is indeed dictated by CaSR. To this end, the plasmalemmal levels of the PtdIns(3,4,5)P_3 biosensor were compared in GM/IFN-γ/LPS– versus M/IL4-cultured macrophages, in the presence and absence of extracellular calcium (Figure 7B), and in the presence of the CaSR antagonist NPS 2143 (Figure 7C). The removal of external calcium markedly reduced plasmalemmal PtdIns(3,4,5)P_3 in the M/IL4-cultured cells, but had only an insignificant effect in the GM/IFN-γ/LPS–cultured cells. Comparable results were observed using NPS 2143, which had a pronounced effect on M/IL4-, but not GM/IFN-γ/LPS–cultured cells. The specificity of NPS 2143 was confirmed by the observation that the antagonist had no effect in HEK 293 cells (unpublished data), which lack CaSR (Canton *et al.*, 2016).

The preceding results suggest that CaSR is more active in M/IL4- than in GM/IFN-γ/LPS–cultured macrophages. We sought to

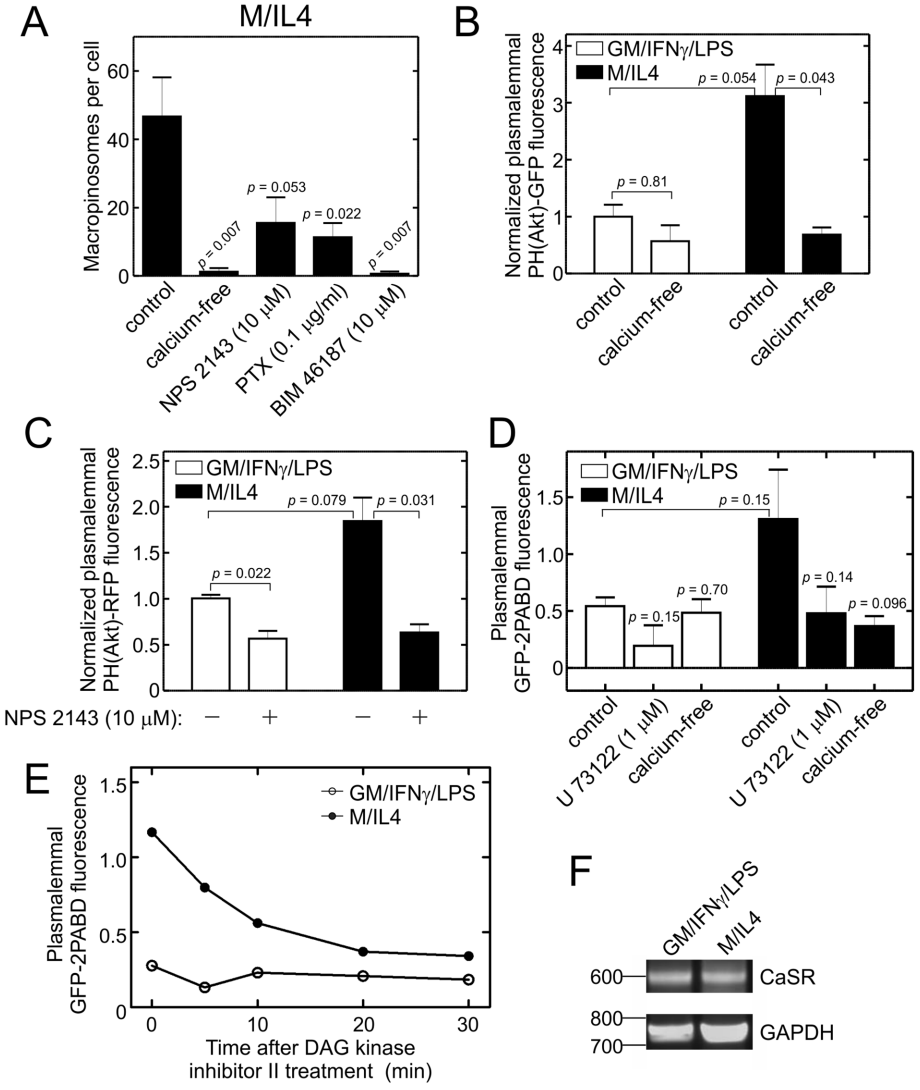

FIGURE 7: Involvement of the CaSR in the differential macropinocytosis of GM/IFN-γ/LPS– and M/IL4-cultured macrophages. (A) M/IL4-cultured macrophages were pretreated with NPS 2143 (10 μM, 30 min), pertussis toxin (PTX; 0.1 μg/ml, 16 h), or BIM 46187 (10 μM, 1 h) and then incubated with fluorescently labeled 70 kDa dextran (TMR-dextran, 125 μg/ml) for 15 min at 37°C, in either calcium-containing (control, NPS 2143, pertussis toxin, and BIM 46187) or calcium-free medium (column 2). Cells were then washed, fixed, and imaged immediately by spinning disk confocal microscopy. The number of macropinosomes (i.e., TMR-positive vacuoles) per cell then was determined as described for Figure 2C. Data are means ± SEM of 30–40 cells from three to four independent experiments of each kind. (B) GM/IFN-γ/LPS– and M/IL4-cultured macrophages were transfected with PH(Akt)-GFP and imaged live 24 h later, in calcium-containing (control) or calcium-free medium. Localization of PH(Akt)-GFP to the plasma membrane was quantified as described for Figure 5B and normalized to the average value for GM/IFN-γ/LPS–cultured cells. Data are means ± SEM of 30–40 cells from five independent experiments. (C) GM/IFN-γ/LPS– and M/IL4-cultured macrophages were transfected with PH(Akt)-RFP and imaged live 24 h later, with or without pretreatment with NPS 2143 (10 μM, 30 min). Localization of PH(Akt)-RFP to the plasma membrane was quantified as described for PH(Akt)-GFP in Figure 5B. Data are means ± SEM of 20–30 cells from three independent experiments. (D) GM/IFN-γ/LPS– and M/IL4-cultured macrophages were transfected with GFP-2PABD, a biosensor of PA and, after 24 h, imaged in calcium-containing medium, with or without pretreatment with 1 μM U 73122 for 1 h, or in calcium-free medium. Localization of GFP-2PABD to the plasma membrane was quantified as described for PH(Akt)-GFP in Figure 5B. Data are means ± SEM of 30–50 cells from three to six independent experiments. (E) GM/IFN-γ/LPS– and M/IL4-cultured macrophages were transfected with GFP-2PABD. After 24 h, individual cells were imaged every 5–10 min for 30 min after addition of DAG Kinase Inhibitor II (R 59949; 30 μM). The localization of GFP-2PABD to the plasma membrane was quantified as in D and plotted as a function of time. A typical time course is representative of three independent experiments. (F) The expression of CaSR mRNA in GM/IFN-γ/LPS– and M/IL4-cultured macrophages was determined by RT-PCR. Expression of GAPDH mRNA was used as a reference. The ethidium bromide gel is representative of four independent experiments. When normalized to GAPDH, the average intensity of bands corresponding to CaSR were not significantly different between GM/IFN-γ/LPS– and M/IL4-cultured cells ($p = 0.26$). Abbreviation: PTX, pertussis toxin.

validate this conclusion by measuring other outcomes of CaSR stimulation. CaSR has been shown to couple to both G_i and G_q proteins (Saidak *et al.*, 2009; Conigrave and Ward, 2013); G_i protein regulates adenylyl cyclase and PtdIns3K, whereas G_q protein activates PLC. By generating diacylglycerol, activation of PLC indirectly stimulates the production of PA. We therefore examined whether the plasmalemmal levels of PA were different between GM/IFN-γ/LPS– and M/IL4-cultured cells, and whether any observed differences were attributable to CaSR, which was assessed by omission of calcium. A biosensor of PA, GFP-2PABD (Bohdanowicz *et al.*, 2013), was expressed in both cell types and its levels at the plasma membrane were normalized to those in the cytoplasm. M/IL4-cultured macrophages had 2.4-fold more plasmalemmal GFP-2PABD than did the GM/IFN-γ/LPS–cultured cells (Figure 7D). Although the difference did not reach statistical significance, it was clear that PA accumulation in the M/IL4-cultured cells was depressed by inhibition of PLC with U73122 (Figure 7D) and also with DAG Kinase Inhibitor II (Figure 7E). Most importantly, accumulation of GFP-2PABD in the membrane of M/IL4-, but not GM/IFN-γ/LPS–cultured cells required extracellular calcium, consistent with formation of PA via CaSR-induced stimulation of G_q.

Next, we examined whether the differential function of the CaSR in the two types of macrophages was due to differential expression; the absence of CaSR in GM/IFN-γ/LPS–cultured cells could readily explain our functional observations. Although available antibodies were not suitable for detection of endogenous CaSR protein by immunoblotting or immunofluorescence, message encoding the receptor was readily detectable in GM/IFN-γ/LPS–cultured cells; its abundance, determined by PCR, was not significantly different from that in M/IL4-cultured cells (Figure 7F). In addition, ectopic expression of CaSR tagged with a fluorescent protein failed to increase constitutive macropinocytosis in the GM/IFN-γ/LPS–cultured

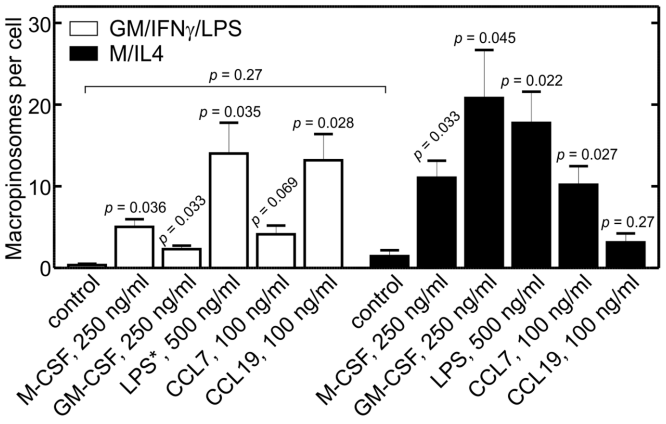

FIGURE 8: Induced macropinocytosis in GM/IFN-γ/LPS– and M/IL4-cultured macrophages in the absence of calcium. GM/IFN-γ/LPS– (white bars) and M/IL4-cultured (black bars) cells were incubated for 10 min at 37°C in calcium-free medium with fluorescently labeled 70 kDa dextran (TMR-dextran, 125 µg/ml), either alone (control) or in combination with M-CSF (250 ng/ml), GM-CSF (250 ng/ml), LPS (500 ng/ml), CCL7 (100 ng/ml), or CCL19 (100 ng/ml). Cells were then washed and imaged live by spinning disk confocal microscopy. In the case of acute LPS treatment of "GM/IFN-γ/LPS" cells (white bars), the asterisk indicates that LPS was omitted from the culture, i.e., the cells in that case were GM/IFN-γ–cultured macrophages. The number of macropinosomes (i.e., TMR-positive vacuoles) per cell then was determined as in Figure 2C. Data are means ± SEM of 27–65 cells from three to four experiments of each type using blood from at least three different donors. Displayed *p* values are for comparisons between the treatment and the control within the same group (i.e., same color of bars), unless indicated otherwise. The size of the macropinosomes varied among treatments; their average diameters were as follows. For GM/IFN-γ/LPS–cultured cells: otherwise untreated control, 1.1 ± 0.2 µm; M-CSF, 2.2 ± 0.6 µm; GM-CSF, 1.1 ± 0.2 µm; LPS, 1.5 ± 0.2 µm; CCL7, 1.4 ± 0.2 µm; CCL19, 3.0 ± 0.8 µm. For M/IL4-cultured cells: otherwise untreated control, 1.0 ± 0.1 µm; M-CSF, 1.7 ± 0.5 µm; GM-CSF, 1.6 ± 0.7 µm; LPS, 1.2 ± 0.2 µm; CCL7, 1.8 ± 0.4 µm; CCL19, 1.4 ± 0.3 µm.

cells (Figure S5A). These observations suggest that GM/IFN-γ/LPS–cultured cells lack essential components to transduce the signal of CaSR and/or to stabilize the functional conformation of the receptor in the membrane.

Acute treatment with cytokines and chemokines induces macropinocytosis in GM/IFN-γ/LPS–cultured cells

While macropinocytosis is negligible in otherwise untreated GM/IFN-γ/LPS–cultured macrophages, we showed earlier that macropinosomes can be formed by these cells when the p85 regulatory subunit of PtdIns3K is forcibly recruited to the plasma membrane (Figure 6). This raised the possibility that receptors other than CaSR may induce macropinocytosis in GM/IFN-γ/LPS–cultured cells. To analyze this possibility we assessed the effects of several agonists on macropinosome formation, comparing their effectiveness in GM/IFN-γ/LPS– and M/IL4-cultured macrophages. These experiments were performed in nominally calcium-free medium, to obviate the contribution of CaSR to macropinosome formation in the M/IL4-cultured cells. When added at 250 ng/ml (a concentration 10-fold higher than that used during differentiation) M-CSF induced significant macropinocytosis in both GM/IFN-γ/LPS– and M/IL4-cultured macrophages, the effects being greater in the latter (Figure 8). Similar effects were observed when a high dose (250 ng/ml) of GM-CSF was added acutely. We also tested the acute response to LPS (500 ng/ml); in this instance, LPS was omitted from the culture during incubation with GM-CSF plus IFN-γ. As shown in Figure 8, LPS markedly stimulated macropinocytosis in both cell types. Lastly, we compared the effectiveness of two chemokines, CCL7 and CCL19, which have been shown to promote chemotaxis differently in pro- and anti-inflammatory macrophages (Xuan *et al.*, 2015). CCL7 induced appreciable macropinocytosis in both GM/IFN-γ/LPS– and M/IL4-cultured cells, although the effect was of borderline significance in the proinflammatory cells (Figure 8). CCL19, on the other hand, induced considerable macropinocytosis in the GM/IFN-γ/LPS–, but not the M/IL4-cultured cells (Figure 8), consistent with its effects on chemotaxis (Xuan *et al.*, 2015). Taken together, these findings support the conclusion that GM/IFN-γ/LPS–cultured macrophages possess a functional and responsive macropinocytic machinery but that, unlike M/IL4-cultured cells, do not perform macropinocytosis in the "resting" state because their constitutive activity of PtdIns3K is minimal.

DISCUSSION

In the present report, we show that blood-derived anti-inflammatory M/IL4-cultured macrophages actively perform constitutive macropinocytosis, while their proinflammatory GM/IFN-γ/LPS–cultured counterparts lack this ability. Differential macropinocytic ability was also observed in macrophages that were cultured under less extreme conditions, but still displayed distinct anti- and proinflammatory properties (Figures 1 and 3). The uptake of large dextrans by the M/IL4-cultured cells was actin and PtdIns3K dependent (Figure 2D), hallmarks of bona fide macropinocytosis (Swanson, 2008; Kerr and Teasdale, 2009). While M/IL4-cultured cells displayed considerably higher expression of Rho-family GTPases, notably Rac1 and RhoG that are thought to support macropinocytosis, this difference is unlikely to account for the inability of GM/IFN-γ/LPS–cultured cells to internalize the dextrans. This conclusion stems from the observation that ectopic overexpression of the wild-type form of the GTPases in GM/IFN-γ/LPS–cultured cells failed to restore macropinocytic activity (Figure 4C). In contrast, the constitutively active forms of Rac1 and RhoG strongly enhanced the macropinocytic activity of the GM/IFN-γ/LPS–cultured cells, reaching levels exceeding those seen in untreated M/IL4-cultured cells (Figure 4E). Moreover, the endogenous levels of the GTPases sufficed to stimulate macropinocytosis when GEFs for Rac1 or RhoG (Tiam1 and sGEF, respectively) were overexpressed. We therefore concluded that insufficient activation—as opposed to limited expression—of the GTPases accounts for the inactivity of GM/IFN-γ/LPS–cultured macrophages. This implies that the machinery downstream from the active Rho GTPases that is necessary for macropinocytosis is available and poised to respond in GM/IFN-γ/LPS–cultured cells.

Our experiments also showed that insufficient activation of the GTPases in GM/IFN-γ/LPS–cultured macrophages correlates with reduced accumulation of PtdIns(3,4,5)P_3 by these cells, which was established using genetically encoded biosensors and also by assessing the phosphorylation state of Akt by immunoblotting (Figure 5, A–C). As in the case of the GTPases, the abundance of PtdIns3 kinases was greater in M/IL4- than in GM/IFN-γ/LPS–cultured cells, but their degree of activation—rather than their density—appeared to be the cause of the reduced level of PtdIns(3,4,5)P_3 in the inflammatory cells. Forced recruitment of the catalytic subunit (Figure 6) confirmed this notion.

The elevated activity of PtdIns3K we observed in M/IL4-cultured macrophages is consistent with previous reports, which show that increased PtdIns3K function is associated with polarization of

macrophages toward the anti-inflammatory, immunosuppressive M2-like phenotype (Wang *et al.*, 2015; Kaneda *et al.*, 2016). Conversely, reduction of PtdIns3K activity by genetic or pharmacological means leads to increased expression of M1 markers and an exaggerated inflammatory response to infection (Kaneda *et al.*, 2016).

Our data further suggest that CaSR activity contributes to the constitutive formation of PtdIns(3,4,5)P_3 in the M/IL4-cultured cells. Heterotrimeric G proteins such as those that transduce the signals generated by CaSR can accomplish this feat, by activating the p110β or p110γ isoforms of PtdIns3K. In this regard, it is noteworthy that macropinocytosis can be induced in other systems (e.g., podocytes) by addition of free fatty acids, which activate G protein–coupled receptors (Chung *et al.*, 2015). Notably, activation of one such receptor, GPR120, by free fatty acids has been shown to activate PtdIns3K through coupling to G_q protein (Oh *et al.*, 2010). It is noteworthy that CaSR activity was not detected in GM/IFN-γ/LPS–cultured cells, despite the presence of mRNA encoding the receptor. The absence of suitable antibodies precluded determination of whether the protein was expressed and properly targeted. It is also conceivable that ancillary proteins required for CaSR function may be absent or inhibited in GM/IFN-γ/LPS–cultured cells. Consistent with this hypothesis, we were able to induce macropinocytosis in the absence of calcium in GM/IFN-γ/LPS–cultured macrophages by activating other receptors that can stimulate PtdIns3K (Figure 8).

Superficially, the impaired constitutive macropinocytic ability of GM/IFN-γ/LPS–cultured macrophages would appear at odds with the well-established stimulatory effect of LPS, the quintessential pyrogen, on macrophages and dendritic cells (West *et al.*, 2004; Zanoni *et al.*, 2011). The solution to this apparent paradox likely lies in the temporal course of events. Indeed, we were able to induce macropinocytosis by acute treatment with LPS (coincident with the 10-min exposure to dextran; Figure 8) of macrophages cultured with GM-CSF and IFN-γ only; like GM/IFN-γ/LPS–cultured macrophages, such cells do not perform constitutive macropinocytosis (Figure 3). A similar acute response to LPS was observed in M/IL4-cultured macrophages in the absence of calcium (Figure 8). These results resemble the reported transient increase in macropinocytosis in response to acute (minutes) stimulation of dendritic cells by LPS, that results in improved antigen uptake. Prolonged stimulation by LPS (hours), however, is accompanied by a dramatic suppression of macropinocytosis (West *et al.*, 2004). The latter situation is more akin to the conditions used in our studies where chronic (2 d) exposure to LPS and IFN-γ was used to generate proinflammatory macrophages, as described by others (Cassatella *et al.*, 1990; Jaguin *et al.*, 2013; McWhorter *et al.*, 2013; Derlindati *et al.*, 2015; Kaneda *et al.*, 2016).

The acute versus chronic effects of LPS, and indeed the differences in the behavior between proinflammatory and anti-inflammatory macrophages, have important functional implications. In immature dendritic cells, as well as in alternatively activated macrophages, macropinocytosis serves for antigen *sampling,* as the phagocytes patrol the tissues. Upon activation by either TLR ligands or proinflammatory cytokines, however, the cells turn to an antigen-*presenting* function. The resulting mature dendritic cells devote their attention to processing the previously captured antigens, and carrying them to the secondary lymphoid organs to be presented to lymphocytes (Liu and Roche, 2015). During this stage, further uptake of antigens is unnecessary and macropinocytosis may in fact be counterproductive, as wholesale membrane internalization would antagonize the retention of presented antigens at the cell surface (Pan *et al.*, 2013; Liu and Roche, 2015), and because cell migration and macropinocytosis appear to be mutually exclusive (Veltman *et al.*, 2014; Veltman, 2015). We propose that suppression of macropinocytosis in proinflammatory macrophages plays a similar role, inasmuch as proteins involved in antigen presentation are expressed preferentially in M1-like cells compared with M2-like cells (Derlindati *et al.*, 2015; Weichhart *et al.*, 2015; Kaneda *et al.*, 2016).

In addition to antigen sampling, macropinocytosis also plays a role in cellular metabolism, a function first identified in amoebae that has been conserved during evolution. Growth factor–induced macropinocytosis in macrophages, for example, delivers amino acids to lysosomes, resulting in increased activation of mTOR (Yoshida *et al.*, 2015). The above-mentioned stimulatory effect of free fatty acids on macropinosome formation (Chung *et al.*, 2015) likely also has an anabolic purpose. In this context, it is worth noting that the polarization of macrophages is accompanied by marked changes in cellular metabolism (Ouimet *et al.*, 2015; Mills and O'Neill, 2016). We are tempted to speculate that the suppression of macropinocytosis contributes to this metabolic switch.

MATERIALS AND METHODS

Reagents

TMR-conjugated 70,000 MW dextran, rhodamine phalloidin, and Lucifer Yellow CH lithium salt were purchased from Life Technologies (Carlsbad, CA). NPS 2143, pertussis toxin, LPS, latrunculin B, rapamycin, and the anti-β-actin monoclonal antibody (mAb) were from Sigma-Aldrich (St. Louis, MO). Wortmannin was from Millipore (Etobicoke, ON, Canada). Paraformaldehyde (PFA; 16% wt/vol) was from Electron Microscopy Sciences (Hatfield, PA). Monoclonal mouse anti-Rac1, anti-RhoA, and anti-Cdc42 antibodies were from the respective G-LISA activation kits (Cytoskeleton, Denver, CO). Monoclonal mouse anti-RhoG antibody (1F3 B3E5) was from Millipore. Rabbit polyclonal anti-p110α, anti-p110β, and anti-p85 antibodies were prepared as described previously (Backer *et al.*, 1992; Yu *et al.*, 1998; Hill *et al.*, 2000). Rabbit monoclonal anti-p110δ (D1Q7R), anti-110γ (D55D5), and anti-phospho-Akt(Ser473) (#9271) antibodies were from Cell Signaling Technology (Danvers, MA). FITC-conjugated anti-human CD40 antibody (5C3), FITC-conjugated anti-mouse immunoglobulin G1 (IgG1) κ isotype (MOPC-21), Alexa-647-conjugated anti-human CD163 antibody (GHI/61), and Alexa-647-conjugated anti-mouse IgG1 κ isotype (MOPC-21) were from BD Biosciences (San Jose, CA). APC-conjugated anti-human CD80 antibody (2D10), APC-conjugated anti-mouse IgG1 κ isotype (MOPC-21), PE-conjugated anti-human CD200R antibody (OX-108), and PE-conjugated anti-mouse IgG1 κ isotype (MOPC-21) were from BioLegend (San Diego, CA). Human recombinant M-CSF, GM-CSF, IFN-γ, IL-4, CCL7, and CCL19 were from PeproTech (Rocky Hill, NJ). EGTA was from BioShop Canada (Burlington, ON, Canada). U73122 was from Tocris Bioscience (Bristol, UK). *Clostridium difficile* toxin B was acquired from TechLab (Blacksburg, VA). HOE 694 was a gift from H. J. Lang (Aventis Pharma, Frankfurt am Main, Germany).

The Superecliptic Phluorin-CaSR (SeP-CaSR) construct was kindly provided by Jeremy Henley (University of Bristol, Bristol, UK). The ELMO-GST construct was a gift from Keith Burridge (University of North Carolina, Chapel Hill). Sources of other plasmids were as follows: GFP (Clontech Laboratories); GFP-Rac1 (Michaelson *et al.*, 2001); GFP-RhoA, GFP-Cdc42, and RhoA-Q63L-GFP were kindly provided by John H. Brumell; GFP-RhoG (Heo *et al.*, 2006); Rac1-Q61L-GFP (Michaelson *et al.*, 2001); Cdc42-G12V-YFP (plasmid #11399; Addgene); RhoG-G12V-CFP was obtained from the laboratory of Tobias Meyer (Stanford University, CA); Tiam1-GFP (plasmid #20154;

Addgene); sGEF-GFP (Ellerbroek *et al.*, 2004); PH-Akt-GFP (Marshall *et al.*, 2001); PH-Akt-RFP (Flannagan *et al.*, 2010); Lyn_{11}-FRB (Marshall *et al.*, 2001); FKBP-p85-CFP (plasmid #20159; Addgene); and GFP-2PABD with nuclear export sequence (Schlam *et al.*, 2013).

BIM 46187 was synthesized as described in Schmitz *et al.* (2014). The forward (5′-CAGGTATAATTTCCGTGGGT-3′) and reverse (5′-GTACTGGGAGATGAGTTCAC-3′) primers for the CaSR reverse transcription-PCR (RT-PCR) and the forward (5′-TTCCAATATGATTCCACCCA-3′) and the reverse (5′-CATACCAGGAAATGAGCTTG-3′) primers for the GAPDH RT-PCR were purchased from Integrated DNA Technologies (Coralville, IA). The GeneJet RNA purification kit and One-Step RT-PCR kit were from Thermo Fisher Scientific (Waltham, MA). The Superscript VILO cDNA synthesis kit was from Life Technologies (Carlsbad, CA). Rac1, RhoA, and Cdc42 G-LISA Activation Assay kits (colorimetric based) were from Cytoskeleton (Denver, CO).

Solutions

The calcium-containing medium was HBSS from Wisent (1.26 mM $CaCl_2$; catalogue number 311-515-CL; MultiCell, St. Bruno, Canada). The calcium-free medium contained 1 mM KH_2PO_4, 154 mM NaCl, 5.6 mM Na_2HPO_4, 2 mM $MgCl_2$, 2 mM EGTA, and 10 mM glucose, pH 7.2 at 37°C.

Macrophage cell isolation, differentiation, and culture

Peripheral blood mononuclear cells were isolated from the blood of healthy donors by density-gradient separation with Lympholyte H (Cedarlane, Burlington, ON, Canada). Monocytes were separated from other mononuclear cells in the washed buffy coat by adherence to tissue-culture–grade dishes at a density of ~4.0×10^7 mononuclear cells per dish. Monocytes were plated in RPMI 1640 supplemented with 10% heat-inactivated fetal bovine serum (FBS) in case they were to be treated with M-CSF only or M-CSF followed by IL-4. In all other cases, monocytes were plated in the absence of serum. One hour after plating the cells, medium was replaced with fresh RPMI 1640 supplemented with 10% heat-inactivated FBS, and antibiotic/antimycotic (MultiCell, Wisent, St. Bruno, Canada) supplemented with either 25 ng/ml human GM-CSF or 25 ng/ml human M-CSF for 5 d, followed by the addition of one, or a combination of, 25 ng/ml IFN-γ, 500 ng/ml LPS, or 25 ng/ml human IL-4, as specified, for another 2 d. The medium and the cytokines were replaced every 2–3 d.

Flow cytometry

Macrophages were gently lifted from tissue-culture plates by incubation with PBS (Ca^{2+}- and Mg^{2+}-free) supplemented with 10 mM EDTA at pH 7.4 for 15 min at 37°C. Cells then were washed three times with 2% bovine serum albumin (BSA; in PBS) and resuspended in 2% BSA (in PBS) at a concentration of ~10^6 cells per 100 µl and labeled with fluorophore-conjugated primary antibodies at the dilution specified by the manufacturer. Cells were incubated for 1 h at 4°C, followed by three washes with cold 2% BSA in PBS and fixation with 2% PFA in PBS; 30 min. Cells then were passed through a cell strainer, run through an LSR II flow cytometer (BD Biosciences, Franklin Lakes, NJ), and analyzed using FlowJo software (Tree Star, Ashland, OR).

Transfections

For human macrophages, DNA transfections were performed using the Neon electroporation system (Life Technologies, Carlsbad, CA). The cells were suspended using Accutase (Life Technologies, Carlsbad) and washed three times. Transfections were performed using the manufacturer's recommended protocol. Transfection efficiency varied from plasmid to plasmid (10–60%); however, only transfected cells were selected for analysis throughout the paper. For HEK293 adherent cells, transfections were performed with FuGENE 6 transfection reagent (Promega, Madison, WI) according to the manufacturer's instructions.

PCR

To detect the expression of CaSR mRNA in macrophages, one-step RT-PCR was performed. RNA was purified from macrophages using the GeneJet RNA purification kit (Thermo Fisher Scientific) and used as a template for the generation of cDNA using the Superscript VILO cDNA synthesis kit (Life Technologies) and subsequent PCR amplification using the One-Step RT-PCR kit from Invitrogen according to the manufacturers' instructions. The primary sequences of the forward and reverse primers are listed in the *Reagents* section. The amplification products were visualized by electrophoresis on agarose gels prestained with ethidium bromide.

Macropinocytosis assay

Cells were suspended using Accutase and plated on 18-mm coverslips 24 h before performing the macropinocytosis assay. In the case of drug treatments, cells were pretreated as follows: HOE 694 (10 µM, 30 min), latrunculin B (2 µM, 30 min), wortmannin (100 nM, 15 min), pertussis toxin (0.1 µg/ml, 16 h), BIM 46187 (10 µM, 1 h), and NPS 2143 (10 µM, 30 min). After pretreatment, the medium was aspirated and replaced with the calcium-containing medium, unless otherwise specified, with TMR-conjugated 70 kDa dextran (125 µg/ml), plus the drug used during the pretreatment. Unless specified otherwise, cells were incubated at 37°C for 15 min and then washed, fixed with 4% PFA and imaged immediately. Imaging was performed by spinning disk confocal microscopy on an Axiovert 200 M equipped with a 63× objective and a separate 1.5× magnifying lens (Carl Zeiss, Oberkochen, Germany). The microscope was fitted with a piezo focus drive and diode-pumped solid-state lasers (440, 491, 561, 638, and 655 nm; Spectral Applied Research, Richmond Hill, ON, Canada). Micrographs were acquired using a charge-coupled device camera (Hamamatsu Photonics, Hamamatsu, Japan) under the control of Volocity software. Macropinosomes were then quantified from the acquired images using the measurement tool in the ImageJ software (Schindelin *et al.*, 2012), either from areas of two-dimensional (2D) particles from projection of three-dimensional (3D) stacks or from volumes of 3D particle analysis from 3D stacks, as specified in the figure legends.

Rac1, RhoA, and Cdc42 activation assays

Rac1, RhoA, and Cdc42 activity was measured with separate colorimetric G-LISA Activation Assay kits (Cytoskeleton, Denver, CO) according to the manufacturer's instructions. In summary, cells were lysed, cellular debris was removed, and the samples were added to the wells of the Rho G-LISA plate coated with Rho-GTP–binding protein on ice. The plate immediately was placed on a shaker for 30 min at 4°C. Then the plate was washed three times at room temperature, and the retained GTP-bound GTPase was probed with either an anti-Rac1, anti-RhoA, or anti-Cdc42 antibody, followed by a secondary antibody tagged with horseradish peroxidase. The signal was measured with a SpectraMax 190 absorbance microplate reader (Molecular Devices, Sunnyvale, CA) at 490 nm after incubation of the well with the detection reagent. The measured absorbance was normalized to total protein levels based on the standard curve obtained with proteins provided with the kit manufacturer.

RhoG activation assay

Differentiated macrophages (day 7) were washed three times with ice-cold PBS and lysed with 500 µl (per 100-mm dish) of 10 mM

$MgCl_2$, 150 mM NaCl, 50 mM Tris, pH 7.4, 1% Triton X-100, 1 mM PMSF, and protease inhibitor cocktail (EDTA-free; cOmplete, Roche). Lysates were cleared at 14,000 × *g* for 10 min. Supernatants were rotated for 30 min with ≈10 µg ELMO-GST (GST fusion protein containing the full-length RhoG effector ELMO) conjugated to glutathione-Sepharose beads (GE Healthcare). Beads were washed in 50 mM Tris, pH 7.4, 10 mM $MgCl_2$, 150 mM NaCl, 1% Triton X-100, and protease inhibitor cocktail. Pull downs and lysates were then subjected to SDS–PAGE (10%) and immunoblotted with an anti-RhoG antibody.

Immunoblotting

Cells were washed three times with ice-cold PBS and subsequently lysed using a small volume of ice-cold RIPA buffer supplemented with protease inhibitor cocktail. Protein concentration was measured using the bicinchoninic acid assay, and 50 µg of protein of each sample was loaded and separated by 10% SDS–PAGE. The protein was transferred to a polyvinylidene difluoride membrane and blocked in Tris-buffered saline (TBS) containing 0.05% Tween-20 (TBST) and 10% fat-free milk for 30 min. The primary antibody was added to the membrane in 5% fat-free milk in TBST for 1 h at room temperature and washed 3 times with TBST for 10 min each. The membrane was reblocked with 10% milk in TBST for 15 min and the HRP-conjugated secondary antibodies were added in 5% milk in TBST for 45 min. The membrane was washed three times with TBST for 10 min each, and the blot was visualized on the Odyssey Fc (LI-COR, Lincoln, NE). Band intensity was quantified using the ImageStudio Lite software.

Data presentation and statistics

Unless otherwise indicated, images are representative of at least three independent experiments, with cells from different donors. Data presented in the text and graphs are the means with standard error of at least three independent experiments, representing the number of total cells as indicated in the figure legends. Unpaired *t* tests were used to establish the significance of experimentally observed differences. Microscopy images were analyzed using ImageJ software (Schindelin *et al.*, 2012) as indicated in the text.

ACKNOWLEDGMENTS

We thank Moshe Kim (The Hospital for Sick Children) for his kind help with purification of ELMO-GST recombinant protein, Jonathan Backer (Albert Einstein College of Medicine) for his generous supply of antibodies to PtdIns3K isoforms, Keith Burridge (University of North Carolina, Chapel Hill) for kindly providing the ELMO-GST construct, and John Brumell (The Hospital for Sick Children, Toronto) for kindly providing the GFP-RhoA, GFP-Cdc42, and RhoA-Q63L-GFP constructs. This work was supported by Grant No. FDN-143202 from the Canadian Institutes of Health Research (CIHR) to S.G. and by Grant No. FOR2372 from Deutsche Forschungsgemeinschaft to M.G.

REFERENCES

Amyere M, Payrastre B, Krause U, Van Der Smissen P, Veithen A, Courtoy PJ (2000). Constitutive macropinocytosis in oncogene-transformed fibroblasts depends on sequential permanent activation of phosphoinositide 3-kinase and phospholipase C. Mol Biol Cell 11, 3453–3467.

Araki N, Johnson MT, Swanson JA (1996). A role for phosphoinositide 3-kinase in the completion of macropinocytosis and phagocytosis by macrophages. J Cell Biol 135, 1249–1260.

Backer JM, Myers MG, Shoelson SE, Chin DJ, Sun XJ, Miralpeix M, Hu P, Margolis B, Skolnik EY, Schlessinger J (1992). Phosphatidylinositol 3′-kinase is activated by association with IRS-1 during insulin stimulation. EMBO J 11, 3469–3479.

Barton GM, Kagan JC (2009). A cell biological view of Toll-like receptor function: regulation through compartmentalization. Nat Rev Immunol 9, 535–542.

Bloomfield G, Kay RR (2016). Uses and abuses of macropinocytosis. J Cell Sci 129, 2697–2705.

Bohdanowicz M, Schlam D, Hermansson M, Rizzuti D, Fairn GD, Ueyama T, Somerharju P, Du G, Grinstein S (2013). Phosphatidic acid is required for the constitutive ruffling and macropinocytosis of phagocytes. Mol Biol Cell 24, 1700–1712.

Canton J, Khezri R, Glogauer M, Grinstein S (2014). Contrasting phagosome pH regulation and maturation in human M1 and M2 macrophages. Mol Biol Cell 25, 3330–3341.

Canton J, Schlam D, Breuer C, Glogauer M, Grinstein S (2016). Calcium-sensing receptors signal constitutive macropinocytosis and facilitate the uptake of NOD2 ligands in macrophages. Nat Commun 7, 11284.

Cassatella MA, Bazzoni F, Flynn RM, Dusi S, Trinchieri G, Rossi F (1990). Molecular basis of interferon-γ and lipopolysaccharide enhancement of phagocyte respiratory burst capability. J Biol Chem 265, 20241–20246.

Chung J, Huber TB, Gödel M, Jarad G, Hartleben B, Kwoh C, Keil A, Karpitskiy A, Hu J, Huh CJ, *et al.* (2015). Albumin-associated free fatty acids induce macropinocytosis in podocytes. J Clin Invest 125, 2307–2316.

Conigrave AD, Ward DT (2013). Calcium-sensing receptor (CaSR): pharmacological properties and signaling pathways. Best Pract Res Clin Endocrinol Metab 27, 315–331.

Das A, Sinha M, Datta S, Abas M, Chaffee S, Sen CK, Roy S (2015). Monocyte and macrophage plasticity in tissue repair and regeneration. Am J Pathol 185, 2596–2606.

Derlindati E, Cas AD, Montanini B, Spigoni V, Curella V, Aldigeri R, Ardigò D, Zavaroni I, Bonadonna RC (2015). Transcriptomic analysis of human polarized macrophages: more than one role of alternative activation? PLoS One 10, e0119751.

De Nardo D (2015). Toll-like receptors: activation, signalling and transcriptional modulation. Cytokine 74, 181–189.

Dowrick P, Kenworthy P, McCann B, Warn R (1993). Circular ruffle formation and closure lead to macropinocytosis in hepatocyte growth factor/scatter factor-treated cells. Eur J Cell Biol 61, 44–53.

Ellerbroek SM, Wennerberg K, Arthur WT, Dunty JM, Bowman DR, DeMali KA, Der C, Burridge K (2004). SGEF, a RhoG guanine nucleotide exchange factor that stimulates macropinocytosis. Mol Biol Cell 15, 3309–3319.

Flannagan RS, Harrison RE, Yip CM, Jaqaman K, Grinstein S (2010). Dynamic macrophage "probing" is required for the efficient capture of phagocytic targets. J Cell Biol 191, 1205–1218.

Gu Z, Noss EH, Hsu VW, Brenner MB (2011). Integrins traffic rapidly via circular dorsal ruffles and macropinocytosis during stimulated cell migration. J Cell Biol 193, 61–70.

Hackstein H, Taner T, Logar AJ, Thomson AW (2002). Rapamycin inhibits macropinocytosis and mannose–receptor mediated endocytosis by bone marrow–derived dendritic cells. Am J Transplant 2, 1084–1087.

Heo WD, Inoue T, Park WS, Kim ML, Park BO, Wandless TJ, Meyer T (2006). $PI(3,4,5)P_3$ and $PI(4,5)P_2$ lipids target proteins with polybasic clusters to the plasma membrane. Science 314, 1458–1461.

Hill K, Welti S, Yu J, Murray JT, Yip SC, Condeelis JS, Segall JE, Backer JM (2000). Specific requirement for the p85-p110α phosphatidylinositol 3-kinase during epidermal growth factor-stimulated actin nucleation in breast cancer cells. J Biol Chem 275, 3741–3744.

Hoeller O, Bolourani P, Clark J, Stephens LR, Hawkins PT, Weiner OD, Weeks G, Kay RR (2013). Two distinct functions for PI3-kinases in macropinocytosis. J Cell Sci 126, 4296–4307.

Holt M, Cooke A, Wu MM, Lagnado L (2003). Bulk membrane retrieval in the synaptic terminal of retinal bipolar cells. J Neurosci 23, 1329–1339.

Jaguin M, Houlbert N, Fardel O, Lecureur V (2013). Polarization profiles of human M-CSF-generated macrophages and comparison of M1-markers in classically activated macrophages from GM-CSF and M-CSF origin. Cell Immunol 281, 51–61.

Jiang Z, Jiang JX, Zhang G-X (2014). Macrophages: a double-edged sword in experimental autoimmune encephalomyelitis. Immunol Lett 160, 17–22.

Kaneda MM, Messer KS, Ralainirina N, Li H, Leem C, Gorjestani S, Woo G, Nguyen AV, Figueiredo CC, Foubert P, *et al.* (2016). PI3Kγ is a molecular switch that controls immune suppression. Nature 539, 437–442.

Kerr MC, Teasdale RD (2009). Defining macropinocytosis. Traffic 10, 364–371.
Li L, Wan T, Wan M, Liu B, Cheng R, Zhang R (2015). The effect of the size of fluorescent dextran on its endocytic pathway. Cell Biol Int 39, 531–539.
Lim JP, Gleeson PA (2011). Macropinocytosis: an endocytic pathway for internalising large gulps. Immunol Cell Biol 89, 836–843.
Liu Z, Roche PA (2015). Macropinocytosis in phagocytes: regulation of MHC class-II-restricted antigen presentation in dendritic cells. Front Physiol 6, 1.
Mantovani A, Biswas SK, Galdiero MR, Sica A, Locati M (2013). Macrophage plasticity and polarization in tissue repair and remodelling. J Pathol 229, 176–185.
Marshall JG, Booth JW, Stambolic V, Mak T, Balla T, Schreiber AD, Meyer T, Grinstein S (2001). Restricted accumulation of phosphatidylinositol 3-kinase products in a plasmalemmal subdomain during Fcγ receptor-mediated phagocytosis. J Cell Biol 153, 1369–1380.
McWhorter FY, Wang T, Nguyen P, Chung T, Liu WF (2013). Modulation of macrophage phenotype by cell shape. Proc Natl Acad Sci USA 110, 17253–17258.
Michaelson D, Silletti J, Murphy G, D'Eustachio P, Rush M, Philips MR (2001). Differential localization of Rho GTPases in live cells. J Cell Biol 152, 111–126.
Mills EL, O'Neill LA (2016). Reprogramming mitochondrial metabolism in macrophages as an anti-inflammatory signal. Eur J Immunol 46, 13–21.
Mosser DM, Edwards JP (2008). Exploring the full spectrum of macrophage activation. Nat Rev Immunol 8, 958–969.
Norbury CC, Chambers BJ, Prescott AR, Ljunggren HG, Watts C (1997). Constitutive macropinocytosis allows TAP-dependent major histocompatibility compex class I presentation of exogenous soluble antigen by bone marrow-derived dendritic cells. Eur J Immunol 27, 280–288.
Oh DY, Talukdar S, Bae EJ, Imamura T, Morinaga H, Fan W, Li P, Lu WJ, Watkins SM, Olefsky JM (2010). GPR120 is an omega-3 fatty acid receptor mediating potent anti-inflammatory and insulin-sensitizing effects. Cell 142, 687–698.
Ouimet M, Ediriweera HN, Gundra UM, Sheedy FJ, Ramkhelawon B, Hutchison SB, Rinehold K, Van Solingen C, Fullerton MD, Cecchini K, *et al*. (2015). MicroRNA-33-dependent regulation of macrophage metabolism directs immune cell polarization in atherosclerosis. J Clin Invest 125, 4334–4348.
Pan H, O'Brien TF, Wright G, Yang J, Shin J, Wright KL, Zhong X-P (2013). Critical role of the tumor suppressor tuberous sclerosis complex 1 in dendritic cell activation of CD4 T cells by promoting MHC class II expression via IRF4 and CIITA. J Immunol 191, 699–707.
Patel U, Rajasingh S, Samanta S, Cao T, Dawn B, Rajasingh J (2017). Macrophage polarization in response to epigenetic modifiers during infection and inflammation. Drug Discov Today 22, 186–193.
Perl A (2016). Activation of mTOR (mechanistic target of rapamycin) in rheumatic diseases. Nat Rev Rheumatol 12, 169–182.
Saidak Z, Brazier M, Kamel S, Mentaverri R (2009). Agonists and allosteric modulators of the Calcium Sensing Receptor and their therapeutic applications. Mol Pharmacol 76, 1131–1144.
Sallusto F, Cella M, Danieli C, Lanzavecchia A (1995). Dendritic cells use macropinocytosis and the mannose receptor to concentrate macromolecules in the major histocompatibility complex class II compartment: downregulation by cytokines and bacterial products. J Exp Med 182, 389–400.
Schindelin J, Arganda-Carreras I, Frise E, Kaynig V, Longair M, Pietzsch T, Preibisch S, Rueden C, Saalfeld S, Schmid B, *et al*. (2012). Fiji: an open-source platform for biological-image analysis. Nat Methods 9, 676–682.
Schlam D, Bohdanowicz M, Chatilialoglu A, Steinberg BE, Ueyama T, Du G, Grinstein S, Fairn GD (2013). Diacylglycerol kinases terminate diacylglycerol signaling during the respiratory burst leading to heterogeneous phagosomal NADPH oxidase activation. J Biol Chem 288, 23090–23104.
Schmitz AL, Schrage R, Gaffal E, Charpentier TH, Wiest J, Hiltensperger G, Morschel J, Hennen S, Häußler D, Horn V, *et al*. (2014). A cell-permeable inhibitor to trap $G\alpha_q$ proteins in the empty pocket conformation. Chem Biol 21, 890–902.
Swanson JA (2008). Shaping cups into phagosomes and macropinosomes. Nat Rev Mol Cell Biol 9, 639–649.
Veltman DM (2015). Drink or drive: competition between macropinocytosis and cell migration. Biochem Soc Trans 43, 129–132.
Veltman DM, Lemieux MG, Knecht DA, Insall RH (2014). PIP_3-dependent macropinocytosis is incompatible with chemotaxis. J Cell Biol 204, 497–505.
Vogel DYS, Glim JE, Stavenuiter AWD, Breur M, Heijnen P, Amor S, Dijkstra CD, Beelen RHJ (2014). Human macrophage polarization in vitro: maturation and activation methods compared. Immunobiology 219, 695–703.
Wang G, Shi Y, Jiang X, Leak RK, Hu X, Wu Y, Pu H, Li W-W, Tang B, Wang Y, *et al*. (2015). HDAC inhibition prevents white matter injury by modulating microglia/macrophage polarization through the GSK3β/PTEN/Akt axis. Proc Natl Acad Sci USA 112, 2853–2858.
Weichhart T, Hengstschläger M, Linke M (2015). Regulation of innate immune cell function by mTOR. Nat Rev Immunol 15, 599–614.
West MA (1989). Distinct endocytotic pathways in epidermal growth factor-stimulated human carcinoma A431 cells. J Cell Biol 109, 2731–2739.
West MA, Wallin RPA, Matthews SP, Svensson HG, Zaru R, Ljunggren H-G, Prescott AR, Watts C (2004). Enhanced dendritic cell antigen capture via toll-like receptor-induced actin remodeling. Science 305, 1153–1157.
Xuan W, Qu Q, Zheng B, Xiong S, Fan G-H (2015). The chemotaxis of M1 and M2 macrophages is regulated by different chemokines. J Leukoc Biol 97, 61–69.
Yoshida S, Pacitto R, Yao Y, Inoki K, Swanson JA (2015). Growth factor signaling to mTORC1 by amino acid-laden macropinosomes. J Cell Biol 211, 159–172.
Yu J, Zhang Y, McIlroy J, Rordorf-Nikolic T, Orr GA, Backer JM (1998). Regulation of the p85/p110 phosphatidylinositol 3′-kinase: stabilization and inhibition of the p110α catalytic subunit by the p85 regulatory subunit. Mol Cell Biol 18, 1379–1387.
Zanoni I, Ostuni R, Marek LR, Barresi S, Barbalat R, Barton GM, Granucci F, Kagan JC (2011). CD14 controls the LPS-induced endocytosis of toll-like receptor 4. Cell 147, 868–880.
Zhou K, Pandol S, Bokoch G, Traynor-Kaplan A (1998). Disruption of Dictyostelium PI3K genes reduces [^{32}P]phosphatidylinositol 3,4 bisphosphate and [^{32}P]phosphatidylinositol trisphosphate levels, alters F-actin distribution and impairs pinocytosis. J Cell Sci 111, 283–294.